Physics and performance of the Alternative Low Power Hybrid Ion Engine (ALPHIE) for space propulsion

IEPC-2019-A-643

Presented at the 36th International Electric Propulsion Conference
University of Vienna, Austria
September 15-20, 2019

L. Conde[*], J. González[†], J.M. Donoso[‡], J.L. Domenech-Garret,[§]
J. Damba, P.E. Maldonado, J. Grabulosa and M.D. Lahoz
Department of Applied Physics. E.T.S. Ingeniería Aeronáutica y del Espacio.
Univ. Politcnica de Madrid 28040 Madrid, Spain

and

M.A. Castillo[¶] J.Casado
VP Technology Development. Aernnova, Miñano, Alava, 01510, Spain

The current status and performance of the ALPHIE plasma thruster is discussed. This new concept was the subject of two recently granted patents and is radically different from conventional (Kauffman) gridded ion engines. Since it makes use of three DC power supplies and only one electron-emitting cathode disposed outside the plasma chamber, its power processing unit has low requisites. This electron emission is employed for both ionization and neutralization of the ion beam. Contrary to usual ion engines where only ions flow through the grids, in this case ionizing electrons and supersonic ions counterflow through the open spaces of a two-grid system. The performance of this plasma thruster was determined using both laboratory tests and particle-in-cell numerical simulations which confirmed the basic physical principles of the ion acceleration process. Laboratory experiments under realistic conditions show the ALPHIE thruster to produce supersonic Argon plasma flows with peak speeds of 37-44 km/s and therefore specific impulses in the range 3700-4400 s^{-1}. Additionally, ALPHIE delivers 1-3.5 mN throtteable thrusts using a maximum 325 W peak power, all of which were directly measured in the laboratory. These performances make ALPHIE suitable for station keeping, flight formation and end-of-life disposal of small and medium sized satellites.

I. Introduction

ELectric propulsion (EP) is necessary for orbital maneuvers of small satellites of the new constellations deployed in the Low Earth Orbit (LEO) intended to provide interactive television services or planetary internet coverage. These in-space propulsive systems are advantageous compared to classical chemical thrusters due to a combination of economic and practical factors.[1–3] They have been used already for orbit raising and station keeping maneuvers as well as in deep-space scientific missions.[4] Nevertheless, their commercial applications have been basically restricted to large telecommunication satellites in geostationary orbit (GEO) due to their high electric power consumption.

[*]Professor, PhD. luis.conde@upm.es.
[†]Aeronautical Engineer, PhD. jorge.gonzalez@upm.es
[‡]Associate professor, PhD. josemanuel.donoso@upm.es
[§]Associate professor, PhD, domenech.garret@upm.es
[¶]PhD. Aeronautical Engineer. miguelangel.castillo@aernnova.com

However, the next generation of small satellites of LEO constellations are being deployed at altitudes where long term interaction with the Earth's atmosphere is not negligible and they will need to be continuously operated to account for the orbital drag force. Their inter-connectivity requires flight formation capability and also a controlled disposal at the end of their operational life. Plasma propulsion is the only technology available so far to achieve the high specific impulses required by the economic rationale of low orbit constellations.

Nevertheless, the size, weight and specifically the reduced electric power available on board are issues that need to be addressed. These small satellites (100-700 kg) require thrusts in the range 0.1-10 mN, with electric power consumption below 500 W. Consequently, low power versions of well established technologies as the Hall Effect Thruster (HET), gridded ion engines (GIE) or the Highly Efficient Multicusp Plasma Thruster (HEMPT) are now under development.[5]

However, new plasma thruster conceptions can also advantageously address these stringent requisites. In this paper we review the performance and current status of the Alternative Low Power Hybrid Ion Engine (ALPHIE) that has been the subject of two recently granted patents.[6,7]

Its principle and basic operation is described in section II and the results of PIC computer simulations supporting its basic physical principles are discussed next in section III. Laboratory measurements of its delivered thrust range using Argon as propellant gas will be introduced in section IV and the structure of the ion velocity distribution function as well as the collimation of the ion beam in V. Finally, we end with some concluding remarks.

II. The ALPHIE plasma thruster

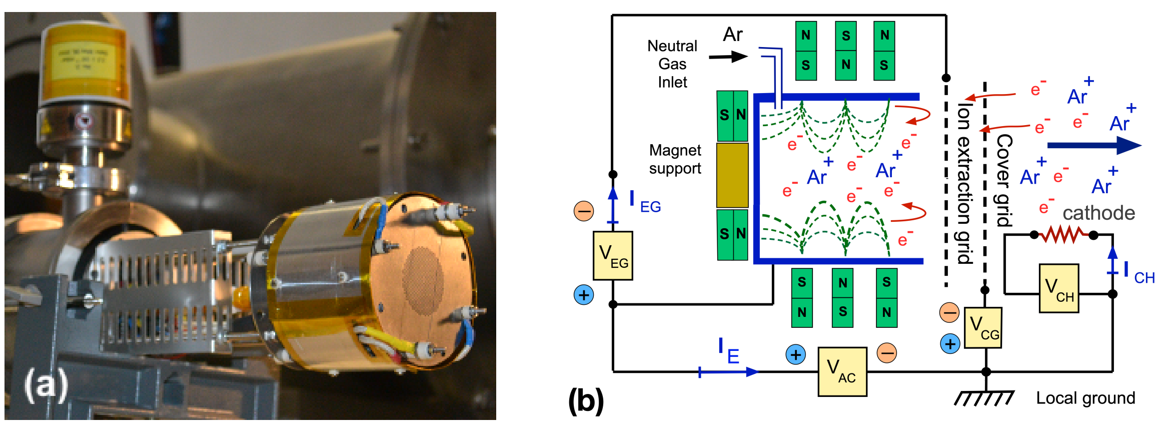

Figure 1. (a) The laboratory prototype of the ALPHIE plasma thruster and (b) the scheme of its longitudinal cross section with the electrical connections.

The small plasma accelerator ALPHIE (10 cm in diameter and 15 cm length) in figure 1a can be regarded as a hybrid conception because it combines elements from other designs. Its operation is discussed in detail in Refs.[8,9] and figure 1b shows a cross sectional scheme of the thruster with its electrical connections.

Briefly, the parallel stainless steel grids have 665 aligned holes of 1 mm diameter and its only electron-emitting cathode is disposed in front of them. Although is can operate with hollow cathodes or other electron emitting devices, a tungsten wire heated by the DC current I_{CH} up to the thermionic electron emission is presently used for simplicity.

In the scheme of Fig. 1 the *extraction* voltage drop $-V_{EG}$ between the metallic wall of the *ionization* or *plasma chamber* extracts ions and repels electrons back. The voltage $(-V_{CG} - V_{AC})$ is applied between the cover grid and the plasma chamber, but V_{CG} is usually set to null in normal operation. Finally, the reference electric potential of the system (local ground) is electrically connected to the cover grid and the electron emitting cathode.

When the external cathode wire is heated up to electron emission temperature, a significant amount of thermionic electrons flow through the open spaces of the grids and are accelerated inwards by the V_{AC} potential towards the ionization chamber. These are trapped inside by the magnetic field configuration and collide with the propellant gas (Argon or Xenon) atoms.

The ions resulting from the electron impact ionization collisions are unmagnetized and as a result are attracted towards the extraction grid. Next, they are accelerated outwards by the V_{AC} voltage between the ionization chamber and the cover grid, and finally, a plasma stream is formed when additional thermionic electrons neutralize the exiting ion flow.

Figure 1b shows the ions moving downstream and the ionizing electrons along the opposite direction, so that the DC *thruster current* $I_E \gg I_{EG}$ represents the counterflow of ions and electrons through the ALPHIE two-grid system in steady state. This constitutes a distinctive characteristic of ALPHIE design; Positive and negative charges flow in opposite directions through the open spaces of the grids.

The ALPHIE's only electron-emitting cathode is responsible for both the ion production and ion beam neutralization, similarly to Hall Effect Thrusters (HET) and Multi-Cusped Field Thrusters (MCFT). No additional cathode is required inside the plasma chamber, contrary to classical (Kaufmann) GIE schemes. This configuration, where positive and negative charges flow through the grids, is radically different from classical GIE schemes where only positive ions move through the open spaces of the grids.

III. Numerical simulations

The previous physical model of ALPHIE operation were confirmed by our numerical simulations using a PIC code. To study the counterflow of particles passing through the thruster grid system, two aligned holes are simulated in a two-dimensional (2D) spatial domain using three-velocity components (3V) of ions and electrons in the axial symmetrical computational domain domain $z \in [0, L_z]$ and $r \in [0, L_r]$ of figure 2a. Argon ions are injected in the upstream boundary and electrons come from the downstream side of the simulation grid as shows the figure 2b.[10] The electron currents from the cathode are $I^e_{IC} + I^e_N$ and $I^e_N = \beta\, I^i_I$ the extracted ion beam and the electron neutralizer current. In the plasma chamber $\alpha\, I^e_{Ic}$, is the ionizing electron current, I^e_s and I^i_I the ion flow. The coefficients $\alpha, \beta < 1$ account for the loss of charges and I_E is the thruster current.

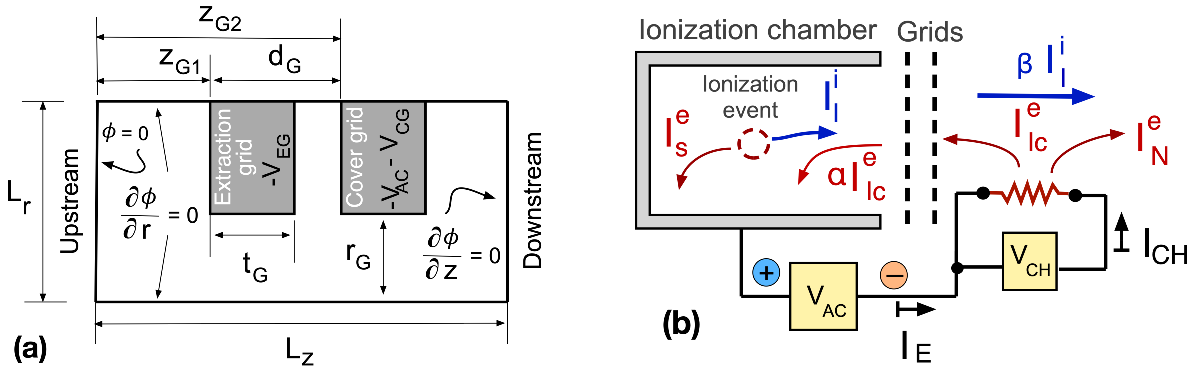

Figure 2. (a) The scheme of the numerical simulation. (a) The numerical domain of the two-grid system with its boundary conditions. (b) The electron ion and currents scheme of numerical simulations

The total injected current is set to $I_h \simeq 110\,\mu$A and the steady electron and ion currents at the downstream and upstream edges are respectively fixed to $I^e_{Ic} \simeq 100\,\mu$A and $I^i_I = 10\,\mu$A. This ion current gives a moderate ionization degree within the ionization chamber between 0.93% and 9.3%, for operation propellant mass flow rates in the range 0.1-1.0 sccm[8] employed in laboratory tests.

Figure 3 shows the typical results of our PIC simulations at $5\,\mu$s when the system has reached a quasi-steady spatial distribution of charged species. The position of the two grids is indicated in the figures by the shaded vertical blocks. In figures 3a and 3b the ion and electron velocities are represented for the radial coordinate $r = 0$ along the Z axis.

In Fig. 3a the ion speed is independent of V_{AC} in the region $0 \le z \le z_{G1}$. The positive charges exit the ionization chamber through the plasma potential profile that develops in front of the upstream face of the extraction grid ($z = 0$–2 mm). The ions are accelerated along $z_{G1} \le z \le Z_{G2} + t_G$ by the electric field established between the extraction and cover grids, that depends on the acceleration voltage V_{AC}.

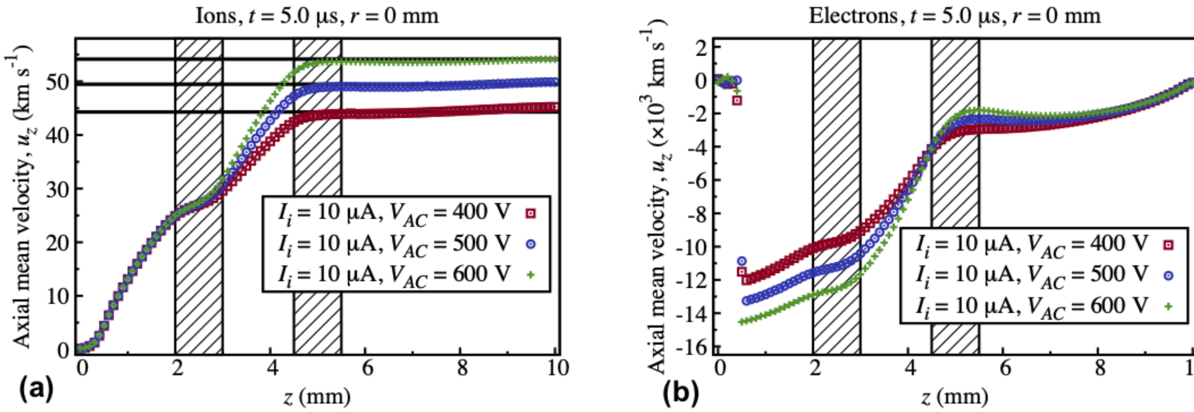

Figure 3. The axial velocity profiles of ions and electrons through the two-grid ALPHIE system for three acceleration voltages V_{AC}. The shaded blocks represent the positions of the ion extraction and cover grids. (a) The ion axial speed is represented with $u_{iz} > 0$ for $r = 0$ where the horizontal solid lines represents the limit exhaust velocities. (b) The axial electron speed of secondary ($u_{ez} > 0$) and ionizing electrons from the cathode ($u_{ez} < 0$) for $r = 0$ is displayed in the figure.

The final velocities of positive particles are in the range $v_i \sim 45$–$55\,\mathrm{km/s}$ whihc are consistent with the applied acceleration potential $v_i \sim \sqrt{2\,e\,V_{AC}/m_i}$ and are also in agreement with the experimental measurements.[8] Finally, the axial ion speed is slightly increased in Fig. 3a for $(Z_{G2} + t_G) < z < L_z$ ($z \sim 6$–$10\,\mathrm{mm}$) by the residual electric field due to the charge imbalance along the downstream zone.

The electrons in Fig. 3b coming from the cathode enter the ionization chamber with very high velocities, in the range $v_e \sim 12$–$15 \times 10^3\,\mathrm{km/s}$ that are equivalent to 400–600 eV electron energies, are also in the order of the applied voltages. These speeds are negative since thermionic electrons move along the opposite direction to that of ions towards the upstream edges, creating the counterflow of charges described above.

These ionizing electrons coexist with the slower secondary electron group I_I^e at the upstream side. These thermionic electrons emitted by the cathode are first slightly accelerated by the low electric field in the downstream zone. Then, they move towards the ionization chamber as they are accelerated to high velocities by the voltage drop between the two grids.

IV. Direct thrust measurements

The thrust delivered by the ALPHIE plasma engine for Argon propellant gas was directly measured using a thrust stand with which provides impulse readings are obtained in the range 0-15 mN with typical absolute errors of $\Delta T = 0.3$ mN and a minimum thrust sensitivity $\delta T_s = 0.3$ mN.[11]

Figure 4 shows the impulse values as a function of the Argon mass flow rates in the range $Q = 0.2 - 0.6$ standard cubic centimeters per minute (sccm) holding constant the acceleration voltage V_{AC}. These impulses are in the range of 0.8-3.5 mN and also shows the throttle capability of the V_{AC} voltage. For a fixed mass flow rate, the delivered thrust is higher when the acceleration voltage increases, as Argon ions reach faster average speeds.

V. Plasma plume structure

The acceleration of plasma ions to supersonic speeds is a key performance of plasma thrusters. Reaching high specific impulses $I_{sp} = v_{ex}/g_o \sim 10^3$ s (g_o is the standard Earth's acceleration) requires of average ion velocities $v_{ex} \sim 10$ km/s, one order of magnitude higher than the characteristic ion sound speed. The thruster exhaust plasma stream is a *mesothermal* flow where ion drift speeds are intermediate between the electron thermal velocity and the plasma ion sound speed.[12,13]

The low energy and supersonic ion groups can be studied in the laboratory using a retarded field energy analyzer (RFEA). This diagnostics provides the ion velocity distribution function (IVDF) in the thruster plasma plume exhaust. It was installed alongside Langmuir and emissive probes on a computer-controlled

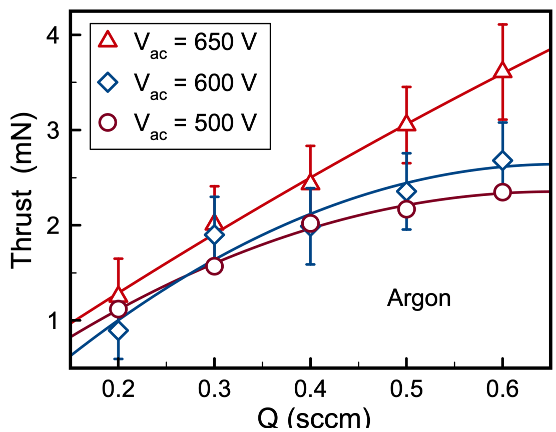

Figure 4. The measured thrusts as a function of the acceleration voltage V_{AC} for Argon propellant gas.

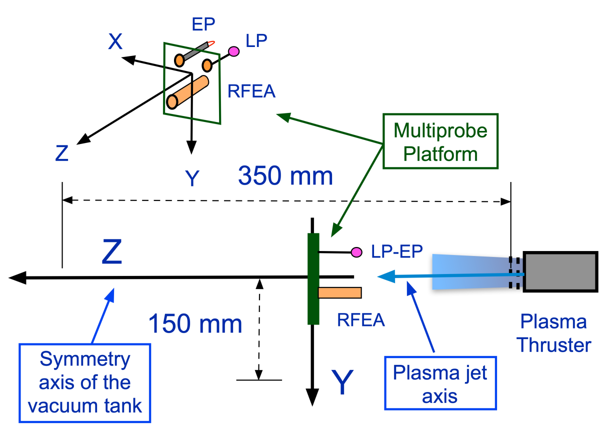

Figure 5. The scheme of the 3D sliding mechanism.

movable platform, driven by three independent stepper motors.

This mechanical system is shown schematically in figure 5 and can displace the platform by up to 300 mm along the Z coordinate axis, coaxial with the symmetry axis of the vacuum tank, and by up to 150 mm along both the X and Y directions. The details of the probes, the experimental data reduction and the 3-D sliding system are discussed in Ref.[9]

The velocity distribution functions of ions at different points of the plasma plume are obtained from the voltage–current characteristic curves of a four-grids RFEA.[9] This diagnostic operates under stationary conditions and its ion-collector current $I_c(V_{id})$ was measured using a Keithley 2000 digital multimeter and a computer-controlled voltage source V_{id} electrically connected to its ion discriminator grid.[14,15] The energy resolution for ions with speeds $u_z > 0$ parallel to the RFEA axis of symmetry was about $\pm$ 8 eV for singly charged Argon ions of 400 eV energy. This is equivalent to radial speeds of $\pm$6 km/s for ions with axial speeds of 44 km/s.

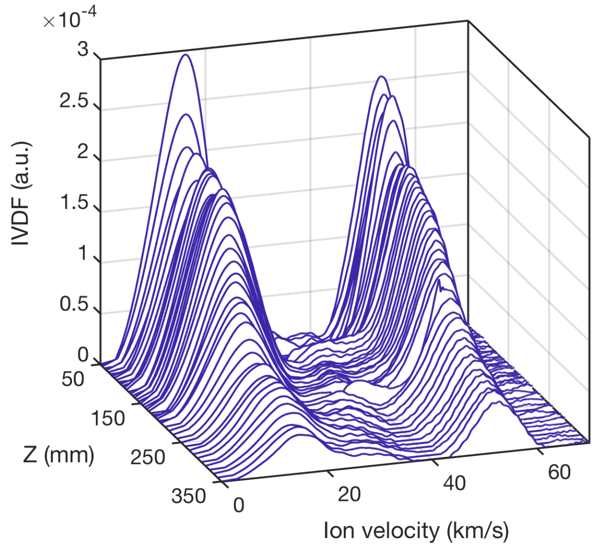

Figure 6. The IVDF measured along the Z axis of the scheme of figure 5. The platform can be displaced along $\Delta X = \Delta Y = 150$ mm and $\Delta Z = 350$ mm.

The platform in figure 5 was used to place the probes within the mesothermal plasma flow generated by our ALPHIE engine. The electron energy distribution function can be considered approximately Maxwellian at a distant point 350 mm away from the plasma thruster. The typical electron densities at this distant point were of $n_e \simeq$ 0.1-8.0 $\times$ 10^8 cm^{-3} with electron temperatures of T_e = 1-2 eV. The electron Debye lengths for this background plasma were of $\lambda_{De} \simeq$ 0.2-0.3 mm.

The probes were later placed close to the exit section of the thruster, in its expanding plasma plume. First, the supersonic ion streams with 37–44 km/s speeds, higher than typical ion sound velocities c_{is} =10–11 km/s were observed at a fixed point 20 cm from the thruster exit section.[8] The emission a high energy ion group by the thruster of along the Z axis of figure 5 was confirmed, as shown in the waterfall representation of the two-peaked IVDFs of figure 6.

Two different ion groups can be observed in figure 6, the slow population has a maximum around $u_{ml} \simeq 15$ km/s whereas the fast ion peak is located at $u_{mf} \simeq 53$ km/s. The velocity distribution of the low energy population is insensitive to the acceleration potential V_{AC}. On the contrary, this acceleration voltage controls the peak energy of the fast ions group, making it operate to as a throttle parameter. When it is incremented (or reduced) it shifts the maximum of the supersonic ion population to higher (or lower) velocities.[8,9]

The shape of the IVDF in figure 6 remains essentially constant over 50–350 mm along the axial direction since throttle potential $V_{AC} = 500$ volts was held constant. However, the heights of maxima decrease with the radial coordinate Z as the plasma stream expands, reflecting the decreasing plasma density along the axial direction.

The estimates of ion temperatures for the two main peaks in 6 give similar values along the Z axis, i.e. $T_{il} = 30$ eV for the low-energy ion group and $T_{if} = 120$ eV for the fast-ion population. Consequently, the fast ion group drifts with a typical supersonic speed of $u_D = u_{mf} - u_{ml} \sim 38$ km/s much higher than the ion sound speed of $c_{is} = \sqrt{k_B(T_i + T_e)/m_i} \sim 8.5$ km/s in this case.

Since the plasma thruster is the only source of ions in our experiment, the interaction of fast positively charged particles with the vacuum chamber walls is the source of the low-energy ion groups in figure 6. The cross sections for elastic and resonant charge exchange collisions of ions with neutral atoms are typically[16,17] $\sigma_{ia} \sim 3 \times 10^{-15}$ cm^2. These give mean free paths of $\lambda_{ai} \simeq 500$ cm for our working pressures and we also have $\lambda_{aa} \simeq 430$ cm for collisions between two neutral Argon atoms.[16] All these mean free paths are much longer than the size of our vacuum vessel.

These considerations exclude the collisional origin of the low velocity ion group, which is produced by the interaction of fast positive particles with the vacuum tank walls. Some recombine after colliding but a fraction is reflected back with reduced velocities pointing along random directions after the interaction. This explains the lack of response of this low energy ion group to thruster operation parameters since they are distributed as a uniform background in steady state. Moreover, charge-exchange collisions between fast ion and non-ionized neutrals also contribute to the group of thermalized ions. On the contrary, fast ions have an important velocity component parallel to the Z axis of figure 5 imparted by the acceleration potential V_{AC}.

The RFEA current voltage-current $I_c(V_{id})$ curve also permits to discriminate the distribution of fast and low energy ions over the transversal cross section of the thruster plasma plume.[9] Figure 7 shows the distribution of the fast ion group from the IVDF of figure 6 over the plasma plume cross section located at $Z = 150$ mm from the ALPHIE thruster exhaust section, using the coordinate system of the scheme 5 and the distances calculated in millimeters.

The sharp peak is located between -20 $\leq X \leq$ 40 and -20 $\leq Y \leq$ 20 and shows that the fast ion beam is approximately located within the area defined by the 40 mm diameter of open spaces of the ALPHIE grids. Therefore, the radial distribution of fast ions of the plasma plume is approximately centered over the projection of the open spaces of the two-grids system and we can conclude that the fast ion group has moderate divergence angles.

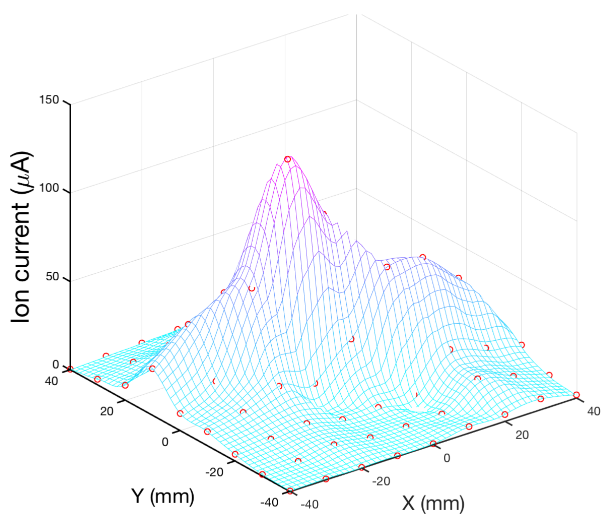

Figure 7. The measurements of the radial distribution of the current of fast ions at point $Z = 150$ mm.

VI. Conclusions

The ALPHIE plasma thruster is a new concept of a gridded ion engine, a subject of two recently granted patents[6,7] whose performance is summarized in table 1. This design makes use of only one electron-emitting cathode and the functionality of its two-grid system is radically different from conventional Kauffman ion thrusters. Both the exiting supersonic ions and the ionizing electrons from its only cathode counterflow through the open spaces of the grids, similarly to HET and Multi-Cusp thruster conceptions. This fact justifies its denomination as a *hybrid* since it incorporates characteristics of different propulsive systems .[8]

Prototypes have been tested in the laboratory under realistic conditions and its modes of operation have been also studied by means of PIC numerical simulations. These have confirmed the basic ion acceleration mechanism as well as the ion and electron counterflow through the ALPHIE two-grid system. This lightweight (below 1.5 kg) and small (10 cm diameter and 15 cm length) plasma thruster makes use of a simple power processing unit of only three DC power supplies.

Magnitude	Value	Commentary
Weight	1.2 kg	Without PPU
Dimensions	10 × 15 cm	
Propellant	Ar, Xe	
Power consumption	200-325 W	
Mass flow $\dot{m}$	1-2 sccm	
Thrust	1-3.5 mN	Ar. Throtteable
Specific impulse I_{sp}	3700-4400 s	
Thrust-to-power ratio	5-11 mN/kW	

Table 1. Performance of the ALPHIE plasma thruster.

The mesothermal plasma plume has supersonic Argon plasma flow peak speeds in the range 37-44 km/s that were determined by laboratory tests from the ion energy spectra and give specific impulses in the range 3700-4400 s^{-1}. The direct measurements of the delivered thrusts give 0.8-3.5 mN for maximum operation voltages of V_{AC}= 650 volts and currents below I_E =500 mA, which represents 325 W peak power consumption.[8,9]

These performances make the ALPHIE plasma thruster a promising new design suited for station keeping, flight formation and/or end-of-life disposal of small and medium sized satellites. Future works will address ALPHIE direct thrust measurements and plasma flow characteristics for Xenon propellant gas. Its performance using more efficient and optimized electron-emitting cathode will be also studied.

Acknowledgments

Authors are grateful to the technical assistance of Mr.F. Sánchez and Mr. J. Damba to the Spanish FPI fellowship program. This work was funded by Aernnova Aerospace S.A. and by the Ministry of Science, Innovation and Universities of Spain under Grant number RT2018-094409-B-100.

References

[1]Goebel, D. M. and Katz, I., *Fundamentals of electric propulsion. Ion and Hall thrusters.*, John Wiley & Sons, Hoboken, New Jersey, USA, 2008.

[2]Charles, C., "Plasmas for spacecraft propulsion," *J. Phys. D: Applied Phys.*, Vol. 42, No. 16, 2009, pp. 163001–1,18.

[3]Ahedo, E., "Plasmas for space propulsion," *Plasma Phys. Control. Fusion*, Vol. 53, 2011, pp. 124037–1,18.

[4]"List of spacecrafts with electric propulsion." 2019, On line; accessed on June 24, 2019.

[5]Mazouffre, S., "Electric propulsion for satellites and spacecraft: established technologies and novel approaches." *Plasma Sour. Sci. Technol.*, Vol. 25, 2016, pp. 1–27.

[6]Conde, L., Domenech-Garret, J. L., Donoso, J. M., Del Río, E., and Castillo, M. A., "Plasma accelerator with modulated thrust." 2019, US patent 10172227B2.

[7]Conde, L., Domenech-Garret, J. L., Donoso, J. M., Del Río, E., and Castillo, M. A., "Plasma accelerator with modulated thrust and space born vehicle with the same." 2015, European Patent EP3369294B1.

[8]Conde, L., Domenech-Garret, J., Donoso, J., Damba, J., Tierno, S., Alamillo-Gamboa, E., and Castillo, M., "Supersonic plasma beams with controlled speed generated by the alternative low power hybrid ion engine (ALPHIE) for space propulsion," *Phys. Plasmas*, Vol. 24, 2017, pp. 123514.

[9]Damba, J., Argente, P., Maldonado, P., Cervone, A., Domenech-Garret, J., and Conde, L., "Multiprobe characterization of plasma flows for space propulsion," *J. Phys. Conf. Ser.*, Vol. 958, 2018, pp. 012002–1,9.

[10]Gonzlez, J. and Conde, L., "Particle-in-cell simulations of the ion extraction and acceleration processes in the alternative low power hybrid ion engine (ALPHIE)," *Physics of Plasmas*, Vol. 26, No. 4, 2019, pp. 043505.

[11]Conde, L., Lahoz, M., Grabulosa, J., Hernández, R., González, J., Delgado, M., and Damba, J., "Low-cost thrust stand based on a sngle point load cell for direct impulse measurments from plasma thrusters," *submitted to Rev. Sci. Instrum.*, 2019.

[12]Zhang, Z., Tang, H., Zhang, Z., Wang, J., and Cao, S., "A retarding potential analyzer design for keV-level ion thruster beams." *Rev. Sci. Instrum.*, Vol. 87, No. 12, 2016, pp. 123510–1,8.

[13]Hu, Y.and Wang, J., "Electron Properties in Collisionless Mesothermal Plasma Expansion: Fully Kinetic Simulations." *IEEE Trans. on Plasma Sci.*, Vol. 43, No. 9, 2015, pp. 2832–2838.

[14]Böhm, C. and Perrin, J., "Retarding-field analyzer for measurements of ion energy distributions and secondary electron emission coefficients in low-pressure radio frequency discharges." *Rev. of Sci. Instrum.*, Vol. 64, No. 1, 1993, pp. 31–44.

[15]Hutchinson, I. H., *Principles of plasma diagnostics.*, Cambridge University Press, New York, USA, 1990.

[16]Raizer, Y. P., *Gas Discharge Physics*, Springer Verlag, Berlin, Germany, 1991.

[17]Lieberman, M. A. and Lichtenberg, A. J., *Principles of Plasma Discharges and Materials Processing.*, John Wiley & Sons,, New York, USA, 1994.